Highly Selective Wet Etch for High-Resolution Three-Dimensional Nanostructures in Arsenic Sulfide All-Inorganic Photoresist

Sean H. Wong,[†,‡] Michael Thiel,[§] Peter Brodersen,[||] Dieter Fenske,[†,‡,#] Geoffrey A. Ozin,[⊥] Martin Wegener,[†,§,#] and Georg von Freymann*[,†,§,#]

Institut für Nanotechnologie, Forschungszentrum Karlsruhe in der Helmholtz-Geminshaft, D-76021 Karlsruhe, Germany, Institut für Angewandte Physik, DFG-Center for Functional Nanostructures (CFN), and Institut für Anorganische Chemie, Universität Karlsruhe (TH), D-76128 Karlsruhe, Germany, Surface Interface Ontario, Department of Chemical Engineering and Applied Chemistry, University of Toronto, 200 College Street, Toronto, Ontario, Canada M5S 3E5, and Materials Chemistry Research Group, Department of Chemistry, University of Toronto, 80 St. George Street, Toronto, Ontario, Canada M5S 3H6

Received March 19, 2007. Revised Manuscript Received June 4, 2007

In this work, we present the rational synthesis of a novel, highly selective etchant, *N*-(4-methoxybenzyl)-(pyren-1-yl)amine, enabling the facile and direct fabrication of free-standing 3D structures within an arsenic−sulfide all-inorganic photoresist, patterned via 3D direct laser writing. The chemical and physical underpinnings of this novel wet etchant are described in detail. Our novel molecule enables the fabrication of intricate, shrinkage-free 3D structures with minimum feature sizes of 180 nm in only one etching step. Because of the high transparency of arsenic−sulfide glass in the telecommunication window, structures fabricated along these lines could be well-suited as final structural elements for 3D optical structures and devices in the sub-micrometer scale. The results presented here enable their facile realization, thus making this material a desirable alternative to traditional photopolymers.

Introduction

Photoresists play a key role in today's fabrication of sub-micrometer structures. Recently, laser lithography entered the third dimension using three-dimensional direct laser writing (3D DLW),[1,2] allowing for rapid prototyping of complex three-dimensional structures. So far, these photoresist structures mainly act as masks or templates for the subsequent deposition or removal of materials, e.g., silicon, which then provide the desired functionality in a combination of shape and materials properties. As this more conventional approach requires several processing steps, it is highly desirable to identify materials and processes that allow for a reduction in process complexity. For photonic applications, arsenic−sulfide (As_2S_3) glasses combine the desired materials properties: they can serve as a photoresist and simultaneously possesses numerous materials advantages, such as a large index of refraction, second-order nonlinear effects, and strong mechanical properties. When this material is combined with the 3D DLW method, functional structures with sub-micrometer resolution can be rapidly generated.[3] However, because of the demanding requirements for fabricating intricate 3D structures with sub-micrometer resolution, a new and novel etchant must be developed in order to enable As_2S_3 to realize the maximum resolution that the 3D DLW method is able to provide.

An important factor for a photoresist to generate large structures with elements possessing sub-micrometer resolution is the selectivity of the developing solution or, the etchant. The selectivity of an etchant (γ) is defined as the ratio between the rate of removal of the unexposed (K_u) and exposed areas (K_e). Therefore, when developing As_2S_3 as a negative-tone photoresist, we should remove the unexposed areas as quickly as possible relative to the exposed areas, so as to afford a large γ, which will allow high-resolution features in thick structures to be produced.

One challenge stems from the fact that 3D structures must be immersed for a longer period of time in the etchant. This is a result of the slower diffusion of liquid etchants though the more tortuous architectures of porous sub-micrometer voids. Another challenge relates to the higher reaction rate on areas that have already been developed by the etchant in 3D microstructures. This is due to the surface area per unit volume of a 3D porous material, being much larger than that of a 3D dense one. Currently available wet-etchants in the literature dealing with As_2S_3 as a photoresist have only been applied to 2D structures less than 500 nm in height.[4,5] Under these circumstances, etch-selectivity requirements are much more relaxed.

* Corresponding author. E-mail: freymann@int.fzk.de.
† Institut für Nanotechnologie, Forschungszentrum Karlsruhe in der Helmholtz-Geminshaft.
‡ Institut für Anorganische Chemie, Universität Karlsruhe.
§ Institut für Angewandte Physik, Universität Karlsruhe.
|| Surface Interface Ontario, University of Toronto.
DFG-Center for Functional Nanostructures (CFN), Universität Karlsruhe.
⊥ Materials Chemistry Research Group, University of Toronto.

(1) Kawata, S.; Sun, H.-B.; Tanaka, T. *Nature* **2001**, *412*, 697.
(2) Deubel, M.; von Freymann, G.; Wegener, M.; Pereira, S.; Busch, K.; Soukoulis, C. M. *Nat. Mater.* **2004**, *3*, 444.
(3) Wong, S.; Deubel, M.; Pérez-Willard, F.; John, S.; Ozin, G. A.; Wegener, M.; von Freymann, G. *Adv. Mater.* **2006**, *18*, 265.
(4) Feigel, A.; Veinger, M.; Sfez, B.; Arsh, A.; Klebanov, M.; Lyubin, V. *Appl. Phys. Lett.* **2000**, *77*, 3221.
(5) Feigel, A.; Veinger, M.; Sfez, B.; Arsh, A.; Klebanov, M.; Lyubin, V. *Appl. Phys. Lett.* **2003**, *83*, 4480.

10.1021/cm070756y CCC: $37.00
Published on Web 07/20/2007

Therefore, in this paper, we describe a rational investigation of an organic solvent-based As_2S_3 etching system, leading to the synthesis of a novel molecule, *N*-(4-methoxybenzyl)-(pyren-1-yl)amine. This molecule allows 3D DLW patterned As_2S_3 to be etched with high selectivity in a simple one-step process. The result of this work enables a new photoresist system to be used for creating fully functional 3D microstructures.

There are two main investigations performed in this study. In the first investigation, a series of systematic synthetic modifications are made to a dibenzylamine molecule. This is done in order to investigate the association between molecular structures and etch selectivity.

In the second investigation, we employed the surface sensitive technique of X-ray photoelectron spectroscopy (XPS) to analyze the surface of etched arsenic−sulfide photoresist films. This analysis aids in the characterization of products formed on the surface before and after the etching reaction, and thus allows the surface chemistry of this particular system to be investigated.

Experimental Section

All chemicals were purchased from Merck KGaA (Darmstadt, Germany), Sigma-Aldrich (U.S.A.), Alfa Aesar (Karlsruhe, Germany), or Lancaster Synthesis (Cambridge, U.K.) and used as received. The identity of the compounds was verified with a 300 MHz ^{1}H NMR, using $CDCl_3$ or $(CD_3)_2CO$ as the solvent. Molecular mass of the compounds was determined using a MALDI-TOF mass spectrometer with ferrulic acid as the matrix.

Procedures for Amine Synthesis. Amine **1** and triethylamine were purchased from Sigma-Aldrich and Merck, respectively, and used without further purification. Unless otherwise indicated, all other secondary amines were synthesized in a general 2 step reaction. The first step consists of formation of imine via the condensation coupling of the respective aldehyde (1 equiv.) and the primary amine or aniline (1 equiv.) in dry ethanol or benzene. Molecules **1**−**15** were synthesized as described previously in the literature.[34−42]

***N*-(4-Nethoxybenzyl)-(pyren-1-yl)amine 16**. A typical reaction is as follows: The above reaction procedure was followed using 4-methoxybenzaldehyde (4.57 mL, 35 mmol) and 1-pyrenecaboxaldehyde (8.06 g, 35 mmol) dissolved in 250 mL of dry benzene and refluxed overnight in a Dean−Stark trap to azeotropically remove water generated from the reaction. $NaBH_4$ (1.6 equiv., 2.12 g, 56 mmol) was used to reduce the amine using methanol as the solvent. This mixture was allowed to stir at 40 °C for 2 h and was then refluxed overnight. At the end of the reaction, the methanol was removed and the remaining solid was first acidified with 1 M HCl and then quenched with 5 wt % $NaHCO_3$ until the solution was slightly basic. The aqueous phase was extracted three times with 75 mL of CH_2Cl_2. The organic phase was then dried using Na_2SO_4, filtered, and the solvent was removed to afford the final amine. The crude products were purified via flash chromatography using silica gel (Kieselgel 60 (0.063−0.200 mm), Merck KGaA) with a mixture of hexane and ethyl acetate. The final product is a light yellow solid. ^{1}H NMR (300 MHz, $CDCl_3$, 25 °C): δ 7.99 (m, 9H, $C_{16}H_9$), 7.3 (d, 2H, $C_6H_4OCH_3$), 6.9 (d, 2H, $C_6H_4OCH_3$), 4.5 (d, 2H, CH_2), 3.9 (d, 2H, CH_2), 3.8 (s, 3H, $C_6H_4OCH_3$). The molecular weight of the solid was determined via MALDI-TOF-MS using Ferrulic acid as the matrix. Calculated $C_{25}H_{21}NO$: 351.4403 g/mol. Found [M + H]: 351.7667 g/mol.

As_2S_3 Photoresist Preparation. Solid As_2S_3 glass of >99.99% purity (Amorphous Materials, Garland, Texas) was used as the precursor material. Silica glass cover-slips (Menzel Gläser, 170 ± 10 μm) were used as substrates. The chalcogenide glass is crushed and then placed in a high vacuum system and thermally evaporated onto the glass substrates, which are mounted onto a water-cooled,

(6) Martin, T. P. *Solid State Commun.* **1983**, *47*, 2, 111.
(7) Mikla, V. I. *J. Phys. Condens. Matter* **1996**, *8*, 429.
(8) Neimanich, R. I.; Connel, G. A. N.; Hayes, T. M.; Street, R. A. *Phys. Rev. B: Condens. Matter Mater. Phys.* **1978**, *18*, 12, 6900.
(9) Zoubir, A.; Richardson, M.; Rivero, C.; Schulte, A.; Lopez, C.; Richardson, K. *Opt. Lett.* **2004**, *29*, 7, 748.
(10) Kolobov, A. V. *Photoinduced Metastability in Amorphous Semiconductors;* Wiley-VCH: Weinheim, Germany. 2003.
(11) Stoycheva, R.; Simidchieva, P.; Buroff, A. *J. Non-Cryst. Solids* **1987**, *90*, 541.
(12) Vlček, M.; Prokop, J.; Frumar, M. *Int. J. Electron.* **1994**, *77*, 6, 969.
(13) Zenkin, S. A.; Mamedov, S. B.; Mikhailov, M. D.; Turkina, E. Yu.; Yusupov, I. Yu. *Glass Phys. Chem.* **1997**, *5*, 393−399.
(14) Mamedov, S. *Thin Solid Films* **1993**, *226*, 215−218.
(15) Voronkov, M. G.; Pizey, J. S. *Reaction of Sulfur with Organic Compounds*; Consultants Bureau: New York, 1987.
(16) Oae, S. *Organic Chemistry of Sulfur*; Plenum Press: New York, 1977.
(17) Davis, R. E.; Nakshbendi, H. F. *J. Am. Chem. Soc.* **1962**, *84*, 2085.
(18) Daly, F. P.; Brown, C. W. *J. Phys. Chem.* **1975**, *79*, 4, 350.
(19) Daly, F. P.; Brown, C. W. *J. Phys. Chem.* **1976**, *80*, 5, 480.
(20) Hodgson, W. G.; Buckler, S. A.; Peters, G. *J. Am. Chem. Soc.* **1963**, *85*, 543.
(21) Mayer, R.; Gewald, K. *Angew. Chem.* **1967**, *79*, 298.
(22) Chen, G. C.; Lauks, I. *J. Appl. Phys.* **1982**, *53*, 10, 6979.
(23) Chen, G. C.; Lauks, I. *J. Appl. Phys.* **1983**, *54*, 5, 2701.
(24) Guiton, T. A.; Pantano, C. G. *Chem. Mater.* **1989**, *1*, 558.
(25) Stec, W. J.; Morgan, W. E.; Albridge, R. G.; van Wazer, J. R. *Inorg. Chem.* **1972**, *11*, 2, 219.
(26) Pratt, A. R.; Nesbitt, H. W. *Am. Mineral.* **2000**, *85*, 619.
(27) Szargan, R.; Schaufuss, A.; Rossbach, P. *J. Electron Spectrosc. Relat. Phenom.* **1999**, *100*, 357.
(28) Molecules containing As−S bonds, such as As_4S_6 and As_4S_4, contain very similar binding energies in their As_{3d} and S_{2p} spectra. In fact, because their binding energies lie so close to each other, the resolution of separate species using conventional XPS may be difficult. Furthermore, other authors, using different characterization methods, have identified all of the species mentioned on the surfaces of as-deposited samples. See: (a) Billes, F.; Mitsa, V.; Fejes, I.; Mateleshko, N.; Fejsa, I. *J. Mol. Struct.* **1999**, *513*, 109. (b) Apling, A. J.; Leadbeater, A. J.; Wright, A. C. *J. Non-Cryst. Solids* **1977**, *23*, 369. (d) Schulte, A.; Rivero, C.; Richardson, K.; Turcotte, K.; Hamel, V.; Villeneuve, A.; Galstian, T.; Vallee, R. *Opt. Commun.* **2001**, 125; and (e) De Neufville, J. P.; Moss, S. C.; Ovhinsky, S. R. *J. Non-Cryst. Solids* **1973**/**74**, *13*, 191. Therefore, we feel that in order give a complete analysis in this current work, it is important to consider and account for all the species that could possibly be present on the surface of our sample. Complementary surface analysis techniques such as time-of-flight mass-spectrometry (TOF-SIMS) may be necessary to clearly elucidate and identify all the species that are present on the surface of these photoresist films.
(29) Schmitz, P. J. *Surf. Sci. Spectra* **2001**, *8*, 3, 195.
(30) Littlejohn, D.; Chang, S.-G. *J. Electron Spectrosc. Relat. Phenom.* **1995**, *71*, 47.
(31) Steudel, R. *Ind. Eng. Chem. Res.* **1996**, *35*, 1417.
(32) Nesbitt, H. W.; Schafuss, A.; Sciani, M.; Höchst, H.; Bancroft, G. M.; Szargan, R. *Geochim. Cosmochim. Acta* **2003**, *67*, 5, 845.
(33) Incorvia, M. J.; Contarini, S. *J. Electrochem. Soc.* **1989**, *136*, 9, 2439.
(34) Blair, K. W.; Tuttle, R. L.; Knick, V. C.; Cory, M.; McKee, D. D. *J. Med. Chem.* **1990**, *33*, 2385.
(35) Anastasi, C.; Hantz, O.; De Clercq, E.; Pannecouque, C.; Clayette, P.; Dereuddre-Bosquet, N.; Dormont, D.; Gondis-Rey, F.; Hirsch, I.; Kraus, J.-L. *J. Med. Chem.* **2004**, *47*, 1183.
(36) Ashton, P. R.; Ballardini, R.; Balzani, V.; Gómez-López, M.; Lawrence, S. E.; Martínez-Díaz, M. V; Montalti, M.; Piersanti, A.; Prodi, L.; Fraser Stoddart, J.; Williams, D. L. *J. Am. Chem. Soc.* **1997**, *119*, 10641.
(37) Hutton, R. C.; Stephen, W. I. *J. Chem. Soc. A* **1967**, 1426.
(38) Paventi, M.; Hay, A. S. *J. Org. Chem.* **1991**, *56*, 20, 5875.
(39) Miriyala, B.; Bhattacharyya, S.; Williamson, J. S. *Tetrahedron* **2004**, 1463.
(40) Samec, J. S. M.; Bäckvall, J.-E. *Chem.—Eur. J.* **2002**, *8*, 13, 2955.
(41) Kim, S. S.; Jung, H. K. *J. Phys. Org. Chem.* **2003**, *16*, 8, 555.
(42) Yu, Z.; Alesso, S.; Pears, D.; Worthington, P. A.; Richard, W. A.; Bradley, M. *J. Chem. Soc., Perkin Trans.* **2001**, *16*, 1947.

Scheme 1. Illustration Showing the Fabrication Process of a Free-Standing 3D "Stepladder" Test Structures in Arsenic−Sulfide-Based Photoresist, Using the 3D DLW Method and Subsequent Wet-Etching

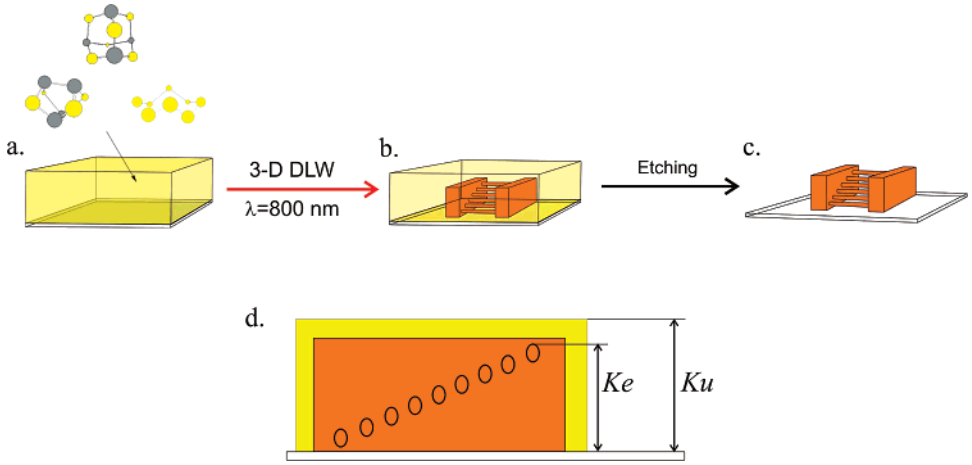

(a) The unexposed photoresist contains As_4S_6, As_4S_4, and S_8 molecules (yellow area). (b) The 3D latent image is already visible inside the photoresist after 3D DLW because of the refractive index increase after writing. (c) The final free-standing 3D structure obtained after removal of the As_4S_6, As_4S_4, and S_8 molecules ysing an etchant solution containing the amine *N*-pyrenyl-*N*-4-methoxybenzylamine **16**. (d) The convention used to define the selectivity is the ratio between the rate of removal of the unexposed area, K_u, and the rate of removal of the exposed area, K_e.

rotating substrate holder directly opposite to the source. The chamber was operated at high vacuum ($P < 2 \times 10^{-6}$ mbar) and the evaporation temperature of the source containing the As_2S_3 precursor was maintained at 390 °C. The entire process is computer controlled to ensure reproducibility. The as-deposited photoresist is orange, optically clear, and transparent. The exact thickness of each individual photoresist film was measured using a fiber interferometer (Mikropak NanoCalc 2000).

3D Photopatterning. Three-dimensional DLW was performed using a regenerative-amplified Ti:Sapphire laser system (Spectra-Physics Hurricane) with a pulse duration of 120 fs. The repetition rate can be computer controlled from 1 kHz to single shots. The wavelength is tuned to 800 nm, where the one-photon absorption of the chalcogenide glass is negligible. The output beam is attenuated by a half-wave plate/polarizer combination and then passed through a quarter-wave plate, and after beam expansion, typically 6 nJ of single pulse energy is coupled into an inverted microscope (Leica). There, the femtosecond pulses are focused into the chalcogenide film by a 100× oil immersion objective with high numerical aperture (NA = 1.4, Leica). The sample is placed on a capacitively controlled three-axis piezo scanning stage, which is operated in closed loop and provides a resolution of better than 5 nm at a full scanning range of 200 μm × 200 μm × 20 μm (Physik Instrumente). A computer controls the scanning operation of the piezo and synchronizes its movements with the output of the laser system.

Etching and Characterization Procedure. All etching and photoresist manipulation were performed under yellow light conditions. The etching was done in atmospheric conditions in a small Petri dish covered with a watch glass, and the film was simply placed in the etchant. The etch time is recorded with a stop watch. To ensure the comparability between different secondary amines, we prepared all etching solutions by dissolving the amine in an otherwise inert solvent system of dimethylsulfoxide (dmso) and 1,2-dichloroethane (1,2-dce) at a concentration of 0.66 M. We chose dmso because it is a solvent that suitably facilitates S_N2 type reactions. The addition of small amounts of 1,2-dce serves as an aid in dissolving larger, less-polar amine molecules.

To develop the exposed films, we placed them in the etchant and periodically removed them. The overall etch selectivity γ is then calculated as the ratio between the rate of removal of the unexposed and exposed areas, K_u and K_e, respectively. To quantify the value of the etch selectivity for each modification step, we use the "stepladder" test structure shown in Scheme 1: 20 μm long rungs are staggered with 250 nm vertical and 2 μm lateral distance. Their ends are attached to two supporting walls. This "stepladder" geometry contains sub-200 nm features, while allowing convenient observation and evaluation of the selectivity via optical microscopy. The removal of the unexposed areas can be visually determined when the color of the photoresist disappears. The removal of the rungs of the ladder is followed with an optical microscope and periodically inspected until the structure is etched to destruction, or if the structure continues to remain, the time is stopped after reaching 72 h (3 days). Inspection of fine surface details, as well as the cross-sections of individual bars, was performed using a scanning electron microscope with a focused ion beam (Ga^+) attachment. All structures characterized using a SEM were first sputtered with 6−8 nm of gold to prevent charging.

X-ray Photoemission Spectroscopy. XPS analysis was performed under UHV conditions, with a Leybold MAX200 spectrometer, using un-monochromated Mg Kα radiation (1253.6 eV) as the excitation source. The energy of the spectrometer was calibrated using the Cu $2p_{3/2}$ (932.7 eV) and Ag $3d_{5/2}$ (368.3 eV) lines. All spectra were collected from an analysis area of 4 × 7 mm^2, under a takeoff angle (TOA) of 20°. The binding energies were calibrated by fixing the C_{1s} neutral carbon peak at (285.0 eV). The peak fitting algorithm provided within the acquisition/analysis software (SPECS GmbH.) was used to fit the data to a series of Gaussian/Lorentzian (80/20%) peaks. Low-resolution scans were made with the analyzer set at 192 eV constant pass energy, and high-resolution scans at 48 eV constant pass energy. The average surface composition was calculated from the low-resolution spectra and normalized to unit transmission of the spectrometer. The surface was analyzed for the elements of arsenic, sulfur, and nitrogen, using the binding energies (BE) of their 3d, 2p, and 1s orbital, respectively. Two different samples were examined: an as-deposited film and a film with a surface passivation layer on its surface. The surface passivation layer was prepared by first photopolymerizing an as-deposited film using a broad-band UV source under a vacuum, in order to avoid air oxidation upon illumination. It is then immersed in an etchant containing amine **16** for 1 h, and finally rinsed with copious amounts of acetone and dried under a stream of nitrogen. These results are shown in Figure 5.

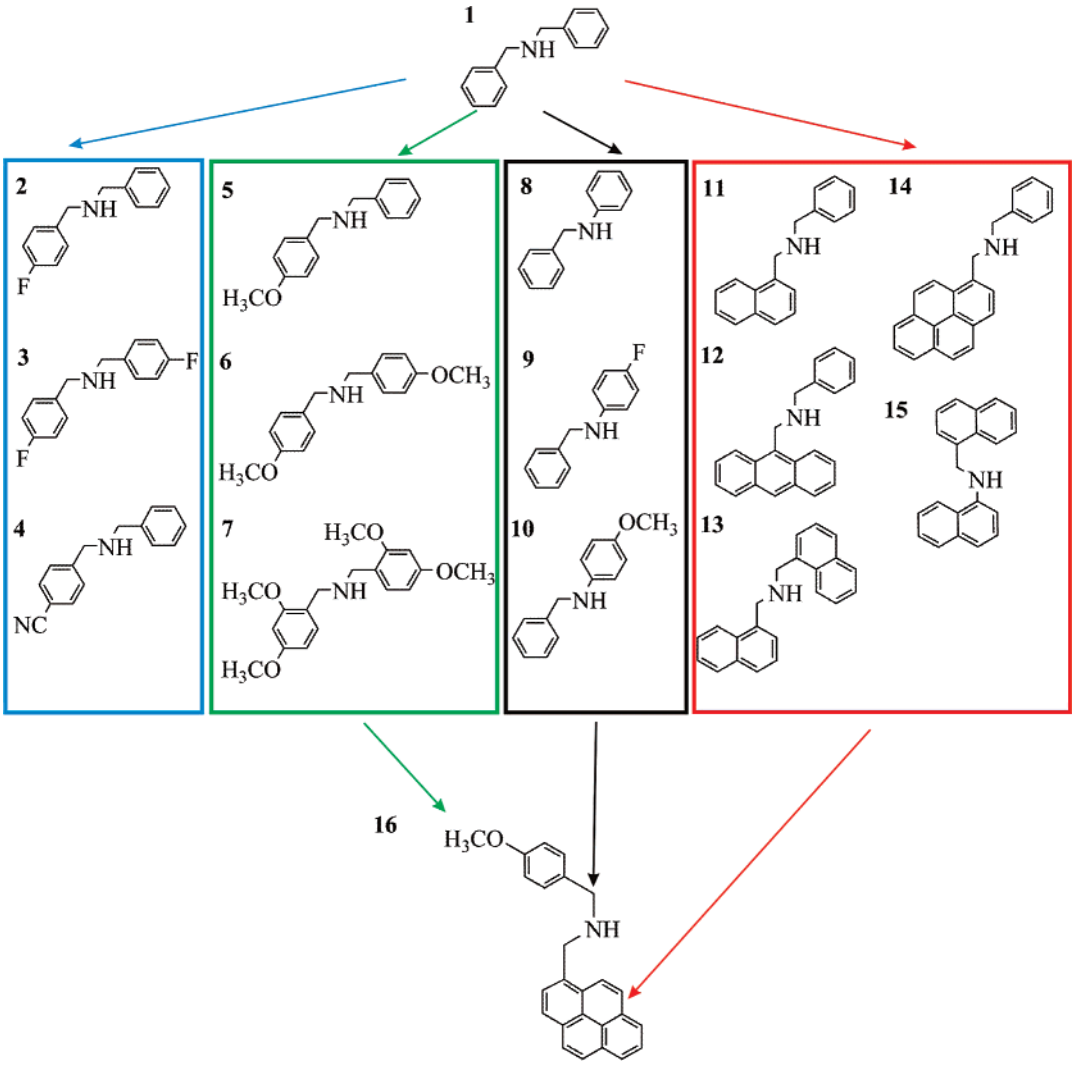

Figure 1. Examples of dibenzylamine derivatives that have been synthesized for this study: the color codes blue, green, black, and red outline the modifications that have been made to amine molecule **1**, namely electron-withdrawing, electron-donating, bridging methylene removal, and steric size increase, respectively. *N*-(4-Methoxybenzyl)-(pyren-1-yl)amine **16** is the resulting amine molecule that embodies all of the desired attributes of each of the modifications.

Results and Discussion

An overview of the processing sequence to produce a 3D structure in As_2S_3 is shown in Scheme 1. To prepare the appropriate phase of As_2S_3 for 3D DLW, we first evaporate the material onto a substrate to form a homogeneous thin film. In the gas phase, a number of arsenic sulfide and sulfur species are present. However, after condensation of the vapor onto the substrate, the products present are the molecules of As_4S_6, As_4S_4, and S_8 (Scheme 2, eq 1).[6−9] These molecules that are present in the as-deposited film are photosensitive, and a photoconversion process essentially photopolymerizes these species back into the heavily cross-linked As_2S_3 glass.[9,10] Once photopatterned, the film is placed into an etchant where only the unexposed areas are removed and can therefore be developed as a negative photoresist.

Reviewing early investigations concerning the solution-phase chemistry of the arsenic−sulfide/sulfur system,[11−14] it was proposed that the reactions between the chemical species on the surface of the film and an amine occurring in polar aprotic organic solvents[13,14] proceed via a series of S_N2 nucleophillic displacement reactions. This series of reactions, occurring in polar aprotic organic solvents, are exemplified in Scheme 2 by eqs 2 and 3. Equation 2 shows that during etching of the unexposed areas, the amine first catalyzes the ring opening of the S_8 molecules that are present in the film.[13] It is well-known that this type of reaction leads to the formation of a complex mixture of charged sulfur species, some of which include anion radicals of sulfur, of various chain lengths, which are highly oxidizing.[15−21] It has been proposed that these highly oxidizing species then serve to oxidize any As−As as well as As−S bonds, thus causing both the molecular species and exposed As_2S_3 to dissolve.[13] Therefore, whether exposed or not, both areas will eventually be removed, leading to a γ too small to be useful for directly etching 3D microstructures.

However, in alternative investigations on the dissolution of the As_2S_3 glass, it was observed that when the reaction is performed using short-chain primary amines as neat solvents, because of the Lewis basicity of the lone electron pair on the nitrogen of the amine, the reaction products found in solution are micellar-like amine and quaternary ammonium cation capped-clusters of As_2S_3.[22−24] This nuclephillic reaction, shown in eq 3 of Scheme 2, was proposed to start at the surface and proceed into the bulk, resulting in subsequent

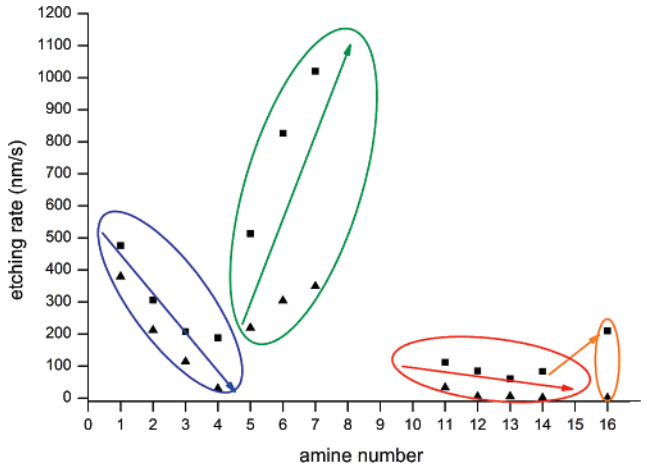

Figure 2. A plot of the K_u (■) and the K_e (▲) of the different amines. The distinct molecular modifications to the dibenzylamine backbone: electron-withdrawing, electron-donating, and steric size effects are marked by the colored circles blue, green, and red, respectively. Arrows indicate the direction of the trends in the etch rates that develop for each modification of the amine. A downward arrow indicates a decrease in the etch rate and vice versa. The orange circle contains optimized amine **16**, which possesses both a sterically large pyrenyl arm and an electron-donating group on the benzyl ring, thus enabling it to realize a larger K_u than its analogue **14**. Amines **8**−**10** and **15** are not plotted on this graph, as these amines showed no reaction when used as the active species in the etchants.

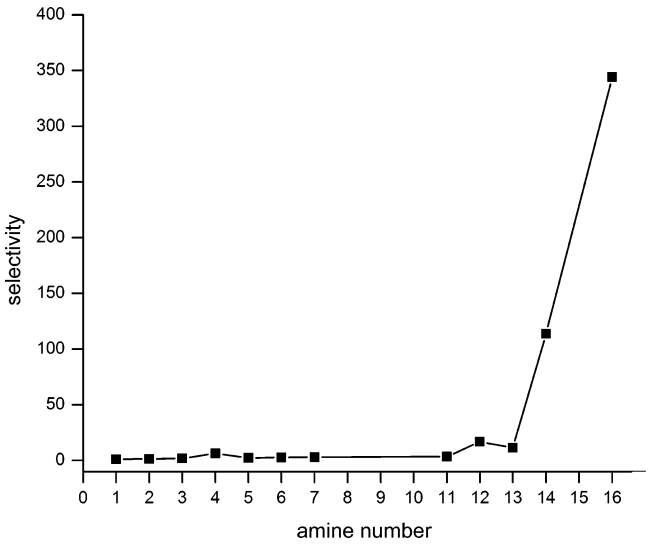

Figure 3. Plot showing the selectivity γ of the different amine molecules synthesized in this study. It can be clearly seen in this graph that there is a dramatic increase in the selectivity as the steric size of the amine increases. Amines **8**−**10** and **15** are not plotted on this graph, as these amines showed no reaction when used as the active species in the etchant.

removal of clusters of the glassy network by the small amine molecules. When the liberated clusters become sufficiently small, its surface becomes completely capped by amine and quaternary ammonium cation molecules. These capping species act to protect the surface from further bond cleavage and oxidation and thus serve to protect the cluster from complete dissolution.

Taken together, these reactions indicate that it may be possible to limit or inhibit oxidizing reactions from occurring at the surface of the exposed areas via the coordination of large amine molecules onto the surface so as to serve as a surface passivation layer. Such an amine must also simultaneously carry out reactions shown in eq 2 of Scheme 2, so as to remove the unexposed areas. The secondary aryl amine molecule, dibenzylamine, was chosen as the synthetic substrate because it is sterically large relative to most primary and short chain secondary amines. Therefore, it should provide an adequate surface passivation layer as a starting point for our investigation.

Etching Results. For the first investigation, 2 systematic series of synthetic modifications are performed on the dibenzylamine molecule. The first series of modifications focuses on changing the basicity of the amine nitrogen via the addition of electron-donating or -withdrawing groups on the benzyl ring. The second series of modifications focuses on increasing the steric demands of the amine molecule via the substitution of the benzyl groups with progressively larger aryl ring moieties. All sixteen dibenzylamine derivatives used in this study are shown in Figure 1. The results of the amine-based etching are summarized graphically in Figure 2 and 3.

On surveying Figure 2, one can identify distinct trends in the etch rates when the dibenzylamine backbone has been modified. Amines **2**−**7** have different electron donating and withdrawing groups attached to the benzyl ring. The dibenzylamine derivatives **2** to **4** that contain electron withdrawing groups are marked within the blue circle. The overall trend, as denoted by the blue arrow, shows a continuous decrease in the etch rate as the strength and the number of electron withdrawing groups increase on the benzyl ring. Amines **5**−**7**, contained within the green circle, have been modified with electron-donating groups. Here, the etch rate increases as the amount of electron-donating groups substituted on the benzyl ring increase. The reason for this behavior can be explained by examining eq 2. Because the generation of the oxidizing sulfur species by an amine is S_N2 in nature,[17,21] the effects of the addition of electron-withdrawing groups serves to slow the etch rates and the addition of electron donating groups has the opposite effect. However, despite providing control of the reaction rates, the graph in Figure 3 shows that these modifications alone do not provide any dramatic increase in the overall etch-selectivity from that of the original dibenzylamine **1**.

Another approach to further increase the etch rates is to remove the $-CH_2-$ bridge between the nitrogen and the phenyl ring. Because the direct linkage between the nitrogen and the phenyl group, this should serve to decrease the steric hindrance of the amine molecule, while at the same time increasing the electronic effectiveness of the substituent groups on the phenyl. These modifications, made in molecules **8**−**10**, shall increase the etch rate of the unexposed areas (K_u), and thus increase the overall selectivity.

However, despite the advantages listed above, these amines exhibit no reaction toward the unexposed areas; the entire film was not etched at all. One plausible explanation could be that this modification increases the steric crowding directly adjacent to the nitrogen atom, thus shielding the nitrogen lone-pair from gaining access to electrophillic sites.[16] Therefore, the inability to catalyze the formation of the oxidizing sulfur species, as shown in eq 2 of Scheme 2, prevents the etching of the unexposed areas. Hence, the conformational limitations of this molecular modification override any

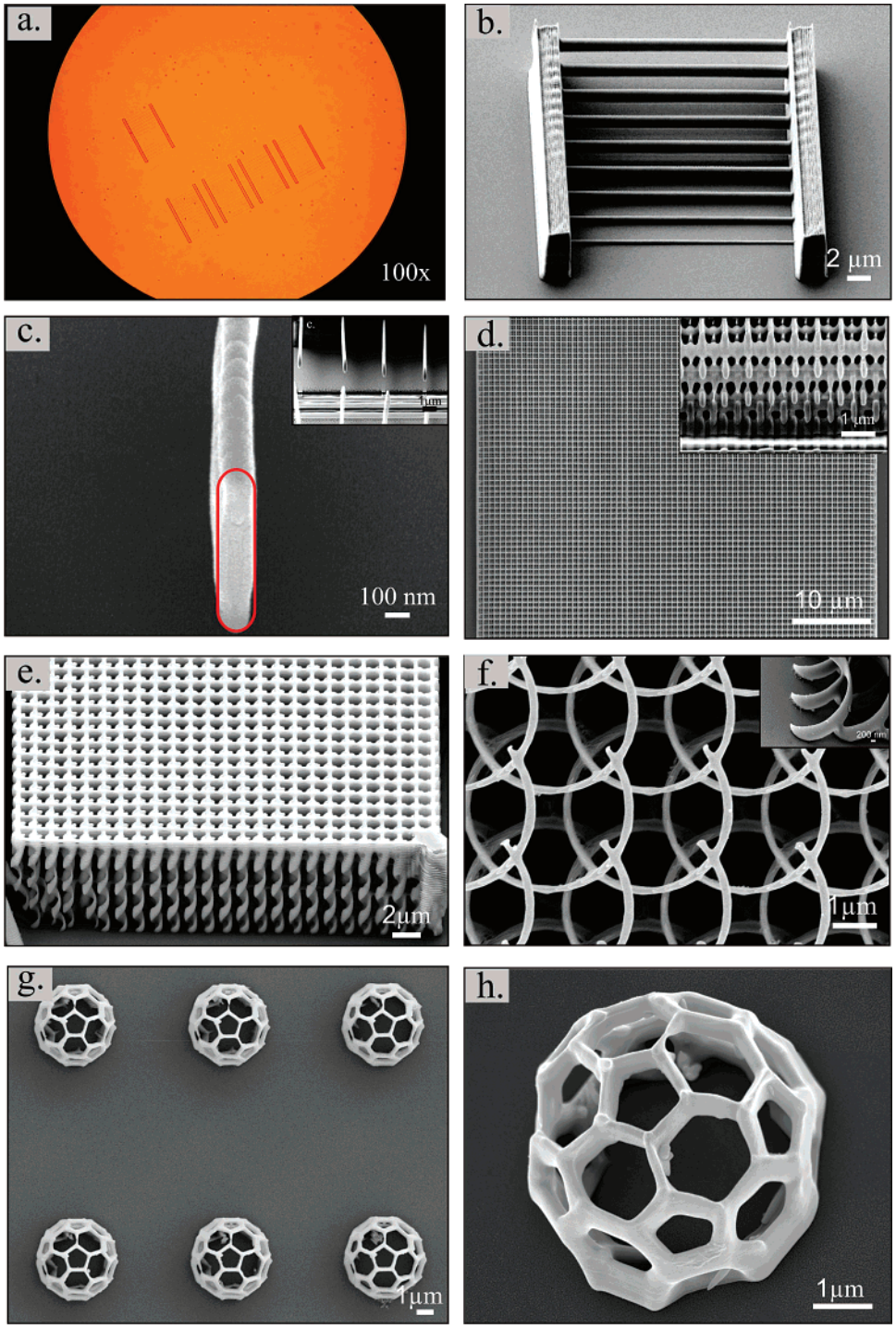

Figure 4. These images show that various 3D As_2S_3 microstructures can be easily fabricated using an etchant-containing molecule (**16**). It is important to note that these structures possess exceptionally smooth close-to-perfect surfaces. Such aspects are critical for highly demanding applications of microstructures, such as those intended for optical applications. (a) Individual rungs of the stepladder test structure are clearly visible before the etching using a light microscope under 500× magnification. (b−g) Three-dimensional microstructures developed with an etchant containing amine (**16**). (b) SEM image of the developed "stepladder" test structure. (c) Close up view of the cross-section of (b) demonstrating that the smallest feature size that is definable using this system is on the order of 180 nm. (d) Three-dimensional woodpile photonic crystal with a lattice constant of 700 nm, and its FIB cross-section (inset). (e) Three-dimensional array of spirals. (f) Top view of a 3D array of fine spirals with individual feature sizes on the order of 180 nm (inset). (g) Array of micro-bucky balls. (h) Close-up of (g) showing a single micro-bucky ball.

benefits to the electronic effects gained using a shorter connection between the nitrogen and the phenyl ring.

We conclude from these observations that electronic modifications alone do not serve to increase the etch selectivity. This could be due to the insufficient steric coverage of the dibenzylamine backbone to effectively passivate the surface of the exposed areas, as was suggested by etching eq 3 in Scheme 2.

To alleviate the deficiency of a lack of steric bulk of the dibenzylamine backbone, the second set of modifications makes a progressive increase to the steric demands of the ring on the benzyl substituent group. In compounds **11**−**14**,

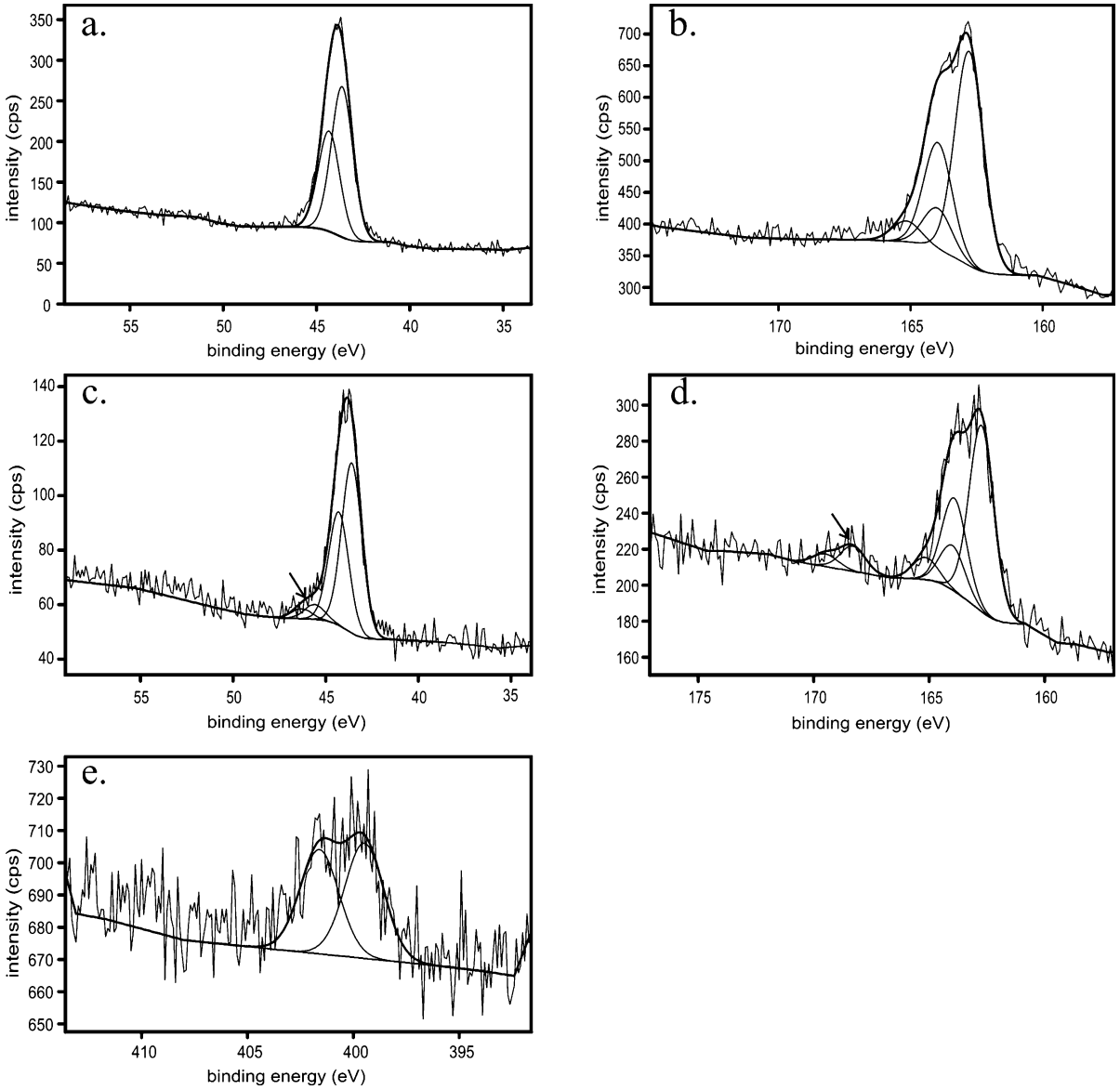

Figure 5. XPS spectra of the surface of thin films of arsenic−sulfide-based photoresist. Spectra of the as-deposited film are shown in graphs for (a) As_{3d} and (b) S_{2p}, and a UV-exposed film that has been immersed in an etchant-containing molecule (**16**), shown in graphs for (c) As_{3d}, (d) S_{2p} and (e) N_{1s}. Black arrows in spectra (c) and (d) indicate new features that arise in the spectra after immersion in the etchant-containing **16** (see main text for discussion).

one arm of the dibenzylamine has been modified by an increasingly larger aromatic moiety. These molecules are highlighted with a red circle in Figure 2. Here, we observed that the K_u and K_e values are much slower compared to **1**. This is due to the restricted exposure of the electron lone pair on the nitrogen as a result of the increased steric hindrance of the larger aryl. However, upon inspection of Figure 3, the etch selectivity tends to increase dramatically as the aromatic group increases in size. In fact, there is almost a 100-fold increase in the etch selectivity on moving from the benzyl-arm of **1** to a pyrenyl-arm of **15**.

Therefore, to further increase the steric bulk of the amine, we synthesize amine **13** by replacing both of the benzyl groups with napthyl groups. As expected, K_u decreases because of the increase in the steric bulk, but the overall selectivity does not improve. A possible explanation is that although the reaction depicted in eq 2 of Scheme 2 is slowed down because of the steric hindrance of the larger aryl groups, they are not large enough to fully passivate the surface from further reaction. This allows the oxidizing species to continue to attack the exposed areas, thus resulting in the total dissolution of the structure.

To further prove that the $-CH_2-$ linkage is required in the amine, regardless of the steric size of the amine, we synthesize amine **15**, an analogue of **13**, but without the $-CH_2-$ linkage between the nitrogen and the aryl ring. No reaction is observed with amine **15**, although etching was observed with **13**. The result obtained here for the sterically large amines is similar to the less sterically hindered amines, **8**−**10**. This reinforces the observation that the presence of a $-CH_2-$ linkage is necessary for the occurrence of the reactions in eq 2 of Scheme 2.

Our series of modifications reveals two main amine design criteria: First, to form an effective passivation layer, it is sufficient to increase the steric size of only one arm of the amine. Second, the extra degree of freedom provided by the

Scheme 2. Chemical Reactions Proposed to Occur during the Different Stages of the Etching Process

Equation 1. $2(m+n)\ As_2S_3 \xrightarrow{\text{high vacuum, } 390\ ^oC} n\ (As_4S_4 + 1/4\ S_8) + m\ As_4S_6$

Equation 2. $R_2NH + S_8 \longrightarrow R_2N{-}S_8{-}H \longrightarrow R_2N{-}S_x\bullet + \bullet S_{8-x}{-}H$

Equation 3. a.

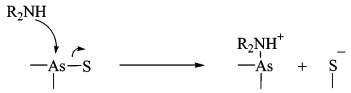

b.

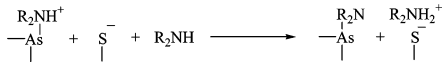

Equation 1 shows the species that are generated during the thermal evaporation of the precursor material. Equation 2 shows the initial steps of a multistep reaction where an amine catalyzes the ring-opening scission of S−S bonds in the S_8 molecules. Equations 3a and 3b show the two reaction steps that take place on the surface of the exposed areas.

methylene linkage is essential for enabling the reaction in eq 2 to occur. Fulfilling both conditions allows the molecule to provide high etch selectivity along the lines of the etching reactions in eq 2 and 3 of Scheme 2.

Although these results even suggest using a tertiary amine for the etching process, this approach fails, as these amines lack the proton on the nitrogen atom. Therefore, the initial proton transfer as required by eq 2 of Scheme 2 does not occur.[16,17] Indeed, when the simple tertiary amine, triethylamine, is used here, the entire photoresist film is not etched at all.

This also explains the results of amine **4**: Because the nitrogen on the cyano side group of **4** does not contain a proton, it cannot serve as a reactive center in a manner depicted in eq 2 of Scheme 2 and thus cannot enhance the K_u. Indeed, this is what we observe. In fact, the K_u observed for amine **4** is even smaller than for the unmodified amine **1**. Furthermore, the slower etch rates obtained by **4** are comparable to those of amine **3**. Thus, the cyano group merely has an electron-withdrawing function and is not an active participant in the etching reaction. The results of the amines etching analysis indicate that the etching follow eq 2 and 3 of Scheme 2.

On the basis of these results, we designed and synthesized a novel molecule, *N*-(4-methoxybenzyl)-(pyren-1-yl)amine **16**, to possess all the attributes required to etch DLW films with high selectivity. In **16**, the bulky pyrenyl-arm, together with an electronic-donating methoxy group on the benzyl ring, act together to provide our best recorded etch selectivity of 344:1. Using the standard concentration solution of **16**, we can routinely produce structures with a minimum feature size of 180 nm. SEM images of optimized test structures developed with **16** are shown in Figure 4

XPS Analysis. The results of the XPS analysis of the as-deposited film (Figure 5 a and b) suggest the presence of molecular species on it surface. In the As_{3d} spectrum (Figure 5a), the position of the BE is consistent with the presence of molecular species containing As−S bonds such as As_4S_4 and As_4S_6. Second, the peaks identified on the S_{2p} spectra (Figure 5b) imply that sulfur is present in both an oxidation state of zero (163.9 eV) and −2 (162.7 eV) and suggests that S_8 is present alongside the As−S containing species. Furthermore, the analysis of the peak areas reveals that the atomic ratio of arsenic to sulfur is 2 to 3, thus indicating that the stochiometry of the precursor is preserved in the as-deposited film. These results obtained here are in good agreement with those found in the literature.[25−28]

Analysis of the film treated with an etchant containing **16** reveals interesting changes on the surface of the film after immersion. In the As_{3d} spectra (Figure 5c), there is an emergence of a new spectral feature at 45.6 eV. Similarly, in the S_{2p} spectra, an additional spectral feature emerges at the BE of 168.3 eV (Figure 5d). It is important to point out that the appearance of these species are not observed on films that have not been treated with the etchant, and no reaction occurs when treated only with the pure solvents. Therefore, this indicates that their presence is a direct result of chemical reactions that have occurred during etching.

The BE of the new feature on the S_{2p} spectra is consistent with sulfate and/or thiosulphate species being present on the surface of the film.[27,29,30] To account for the presence of sulfate or thiosulphate species on the surface, we should begin by mentioning that polysulfide anions, similar to those generated from the amine-catalyzed reactions shown in eqs 2 and 3 of Scheme 2, are known to undergo rapid auto-oxidation into sulfate and thiosulphate in many industrial processes where wet oxidization is employed.[31] Furthermore, the new spectra feature in the As_{3d} spectra (Figure 4c) are also consistent with the presence of arsenic oxides.[32]

Because the highly selective etchant used here is prepared and used under atmospheric conditions without the need for any special apparatus or dry solvents, traces of water and oxygen will undoubtedly be present. It is likely that this is the reason for oxidation products to be observed on the surface of the films treated with the etchant. Despite these products of oxidation being present, SEM images of the 3D microstructures produced here (Figure 4) show that their influence is limited as the final surfaces remain smooth and defect free.

We obtained further information upon inspection of the N_{1s} spectra (Figure 5e). There, two distinct signals suggest the presence of different nitrogen atomic environments in the −3 oxidation state. The first signal at 401.6 eV is consistent with nitrogen present as the ammonium cation,[30] and the second signal at 399.5 eV with the presence of an As(+3)−N(−3) direct bond.[27,33] The identification of these species are in line with the expected reaction products of eq 3 of Scheme 2. Furthermore, the second result here implies that another arsenic species besides the oxide exists on the surface. Namely, the new feature in the As_{3d} spectra (Figure 4c) at the BE of 45.6 eV is also consistent with a +3 oxidation state of an organo-arsenic species. This observation was not immediately obvious in the As_{3d} spectra, because both arsenic oxides and the organo-arsenic species possess similar binding energies.[25]

Previous literature investigating etching mechanisms of As−S-based photoresists do not take into account of the effects of atmospheric water and oxygen in their analy-

sis.[13,14,22,23] From the XPS results presented here, it seems that their presence, along with amine **16**, produces reaction products that were previously unexpected. Furthermore, because the generation of the species observed here can be accomplished via different reaction pathways, the etching mechanism maybe much more complex than previously indicated. The analysis performed here suggests the presence of a mixed-surface passivation layer and various oxidation products, providing possible new insights into the etching mechanism. Future works entail a further study of the surface of photoresist films using other surface-sensitive techniques and elucidation of the reaction mechanism under rigorously controlled reaction conditions.

Conclusion

A series of aryl amines has been synthesized, and their wet-etching behavior has been systematically investigated using As_2S_3 photoresist films structured via 3D DLW. The results of this investigation guided us to the design and synthesis of a novel *N*-(1-pyrenyl)-(4-methoxybenzyl)amine, which enabled a 3D etch selectivity of 344:1 and feature sizes as small as 180 nm. An analysis of the surface using XPS suggests the presence of a mixed-surface passivation layer and various oxidation products, providing possible new

Acknowledgment. We acknowledge the support by the Centre for Functional Nanostructures (CFN) of the Deutsche Forschungsgemeinschaft (DFG) within project A.1.4. The research of G.v.F. is further supported by DFG-project FR 1671/4-3 (Emmy-Noether program) and that of M.W. by We 1497/9-1. G.A.O. is a Government of Canada Research Chair. We are grateful to the Natural Science and Engineering Research Council of Canada (NSERC) for financial support of this work, and Dr. S.T. Balaban, S. Vanneste, and Dr. G. Zoppellaro for insightful discussions regarding organic synthesis techniques.

Supporting Information Available: ^{1}H NMR and MS data, as well as a tabulated etch rates, of the amine molecules synthesized and used here. This material is available free of charge via the Internet at http://pubs.acs.org.

CM070756Y